Original Article

DOI: 10.5582/ddt.2025.01061

Piezo1 mediates calcium ion influx, glucose transporter 4 translocation, and glucose uptake in adipocytes under low-frequency vibration

Dazhuang Huang[1,2], Daijiro Haba[3,4], Sanai Tomida[1,2], Chihiro Takizawa[1], Qi Qin[1], Yukie Kataoka[1], Yuko Mugita[1,2], Hiromi Sanada[5], Gojiro Nakagami[1,4,*]

[1] Department of Gerontological Nursing/Wound Care Management, Graduate School of Medicine, The University of Tokyo, Tokyo, Japan;
[2] Department of Next-generation Wound Care Innovation, Graduate School of Medicine, The University of Tokyo, Tokyo, Japan;
[3] Department of Well-being Nursing, Graduate School of Nursing, Ishikawa Prefectural Nursing University, Ishikawa, Japan;
[4] Global Nursing Research Center, Graduate School of Medicine, The University of Tokyo, Tokyo, Japan;
[5] Ishikawa Prefectural Nursing University, Ishikawa, Japan.

SUMMARY: Diabetic foot ulcers (DFUs) are associated with a high risk of amputation and mortality, necessitating effective wound-healing interventions. Low-frequency vibration (LFV) therapy promotes wound healing by increasing glucose metabolism; however, the mechanisms underlying the effects of LFV on glucose metabolism remain unclear. This study aimed to investigate the role of Piezo1 in glucose uptake induced by LFV in adipocytes. 3T3-L1 adipocytes were subjected to LFV (52 Hz, 600–1,000 mVpp, and 40 min/day) for five days. Cells were divided into non-LFV and LFV groups, both with or without the Piezo1 inhibitor, which was evaluated for intracellular (Ca^{2+}) fluorescence intensity, glucose transporter 4 (GLUT4) localization, and glucose uptake. The increased intracellular Ca^{2+} fluorescence intensity induced by LFV was significantly attenuated when combined with Piezo1 inhibitor ($p < 0.0001$). LFV-induced GLUT4 translocation to the plasma membrane was canceled, and glucose uptake was significantly decreased in the LFV group treated with Piezo1 inhibitor ($p < 0.001$) compared to the LFV group without Piezo1 inhibitor. The activation of Piezo1 by LFV may lead to a cascade involving Ca^{2+} influx, GLUT4 translocation, and increased glucose uptake. These findings suggest that Piezo1 plays a critical role in promoting the glucose uptake induced by LFV in adipocytes.

Keywords: Diabetic foot ulcers, GLUT4, glycometabolism, hard-to-heal wounds, mechanosensors

1. Introduction

The prevalence of diabetes is substantially increasing, driven by lifestyle and social changes (*1*). According to the International Diabetes Federation, the number of people with diabetes was 537 million in 2021, equating to one in every ten adults (*2*). Diabetes is an incurable metabolic disorder characterized by chronic hyperglycemia, which is due to insulin resistance, severely impacting people's quality of life and placing growing economic and medical burdens on society, particularly in those with aging populations (*3-5*). Prolonged hyperglycemia causes extensive cellular damage, leading to complications such as retinopathy, nephropathy, and neuropathy. DFUs are a particularly debilitating complication associated with underlying neuropathy and vascular damage; DFUs are challenging to treat effectively (*6,7*). The estimated lifetime cumulative incidence of DFUs among people with diabetes is 19–34%, with an annual incidence of approximately 2% worldwide (*8*). Recurrence rates within one year of healing are 30–40% (*9*).

The current treatments for DFUs include exercise, pharmacotherapy, dietary interventions, and glycemic control (*10-12*). However, maintaining glycemic control poses significant challenges, and poor patient adherence to treatment often leads to treatment failure and hard-to-heal wounds. Chronic hyperglycemia-induced vascular damage reduces the flow of blood to wounds, impairing the healing of DFUs (*5*). Therefore, promoting blood flow and restoring circulation are critical for effective DFU management.

Local low-frequency vibration (LFV) is a novel non-invasive wound care for enhancing blood circulation and promoting wound healing. Local LFV has been shown to increase blood flow through nitric oxide (NO)-mediated vasodilation and has been used to effectively treat full-thickness wounds in animal studies (*13-15*). Although

NO synthesis is impaired under diabetic conditions due to chronic hyperglycemia (*6*), clinical research has validated that vibration devices placed under mattresses facilitate the healing of DFUs (*16*). In our previous study, we found that LFV benefits the wound healing of DFUs by increasing local glucose metabolism *via* the AMP-activated protein kinase (AMPK)-mediated translocation of GLUT4 to the plasma membrane, thereby promoting wound healing under high-glucose conditions (*17,18*). However, the precise mechanisms underlying the LFV-induced enhancement in glucose uptake remain unclear. Identifying these molecular pathways is critical for optimizing LFV application in DFU treatment and minimizing its potential adverse effects. A deeper understanding of these mechanisms is essential for advancing the implementation of LFV as a therapeutic measure.

In our previous study, we found that the promotion of glucose uptake induced by LFV was closely associated with the influx of Ca^{2+} (*19*). The Ca^{2+} influx induced by mechanical stress is typically mediated by mechanosensors. Mechanosensors are specialized cellular structures or proteins that detect mechanical stimuli, such as vibration, pressure, stretch, or shear stress. Mechanosensors convert these physical forces into biochemical or electrical signals (*20*), playing critical roles in enabling cells and tissues to respond to changes in their mechanical environment. Piezo1 is a mechanosensitive ion channel; a type of protein embedded in cell membranes, that plays a key role in detecting and responding to mechanical stimuli such as vibration (*21*). Piezo1 opens its channels when activated by these forces to allow the influx of positively charged ions such as Ca^{2+} into the cell (*22*). Based on these findings, the following hypothesis was considered: the promotion of glucose uptake induced by vibration would be associated with the activation of Piezo1.

As such, the aim of this study was to elucidate the role of Piezo1 in promoting the LFV-induced glucose uptake in adipocytes, thereby clarifying the molecular mechanisms through which vibration therapy facilitates the healing of DFUs.

2. Materials and Methods

2.1. Cell culture

The 3T3-L1 cells were obtained from the Japanese Collection of Research Resources Cell Bank (Osaka, Japan). The cells were seeded in a culture plate or chamber slide and cultured in low-glucose Dulbecco's modified Eagle's medium (DMEM; FUJIFILM Wako Pure Chemical Corporation, Osaka, Japan) supplemented with 10% (v/v) heat-inactivated fetal bovine serum (FBS; Cytiva, Marlborough, MA, USA) and 5% (v/v) penicillin-streptomycin (PS) solution (Nacalai Tesque, Kyoto, Japan) until confluence was reached (day 0). After reaching confluence, the cells were cultured for three days in low-glucose DMEM containing 10% FBS, 5% PS, 10 μg/mL insulin (FUJIFILM Wako Pure Chemical Corporation), 1 μM dexamethasone (FUJIFILM Wako Pure Chemical Corporation), and 0.5 mM 3-isobutyl-1-methylxanthine (FUJIFILM Wako Pure Chemical Corporation) (day 3). Subsequently, the cells were maintained in low-glucose DMEM with 10% FBS, 5% PS, and 10 μg/mL insulin for an additional three days (day 6). Finally, the cells were transferred to high-glucose DMEM containing 10% FBS and cultured for two more days (day 8). Fully differentiated 3T3-L1 adipocytes (day 9–13) were used in the experiments.

2.2. Adipogenesis assay using oil red O staining

Oil Red O staining was performed to confirm that the differentiation of the adipocytes was successful. This staining method, which is commonly used to evaluate adipocyte differentiation, selectively stains the lipid droplets within cells. The amount of dye extracted from the stained droplets correlates with the volume of accumulated lipids. The treated adipocytes were fixed in 10% formalin, and intracellular lipid droplets were stained using an Oil Red O Stain Kit (Cosmo Bio, Tokyo, Japan). Staining and dye extraction assays were performed according to the manufacturer's instructions. Observations were conducted using a bright-field microscope (Leica CTR 4000, Leica Microsystems, Wetzlar, Germany), and the absorbance of the extracted dye was measured at 540 nm using a plate reader (SpectraMax iD3, Molecular Devices, San Jose, CA, USA).

2.3. Real-time reverse-transcription polymerase chain reaction (RT-PCR)

RT-PCR was used to evaluate the gene expression level of *Piezo1* in 3T3-L1 adipocytes. Complementary DNA (cDNA) was synthesized using a high-capacity cDNA Reverse Transcription Kit (Thermo Fisher Scientific, Waltham, MA, USA) with random primers. The target cDNA was amplified using an Mx3000P QPCR System (Agilent Technologies, Santa Clara, CA, USA). *Piezo1* TaqMan® Gene Expression Assay (Mm01241549_m1, Thermo Fisher Scientific) was used. The real-time RT-PCR program was set as follows: 50°C for 2 min, 95°C for 10 min, followed by 50 cycles at 95°C for 15 s, and 60°C for 1 min. All samples were tested in triplicate.

2.4. Vibration profiles and experimental set-up

Four groups were designed to verify our hypothesis: an LFV group with and without the Piezo1 inhibitor and a non-LFV group with and without the Piezo1 inhibitor. The vibration settings were as follows: a DC-regulated power supply (AD-8735, A&D, Tokyo, Japan) and

four miniature vibration motors (C1034, SHICOH, Kanagawa, Japan) connected in a parallel circuit were used to generate vibration according to a previous study (*17*). The vibration intensity was changed by adjusting the voltage of the power supply. For LFV groups, LFV was applied at 52 Hz and 600–1,000 mVpp for 40 min per day to the 3T3-L1 adipocytes from day 9 to 13 after differentiation, with the medium and the Piezo1 inhibitor Grammostola spatulata mechanotoxin 4 (GsMTx4; Adooq Bioscience, Irvine, CA, USA) replaced daily (*23*). For with Piezo1 inhibitor groups, GsMTx4 was added to each well 4 h before vibration. For 6-well plates, 10 µL of a 200 µM GsMTx4 solution in 0.9% NaCl was added to each well, and for 96-well plates, 5 µL of a 40 µM GsMTx4 solution in 0.9% NaCl was added to each well. In both cases, the final concentration of GsMTx4 was 1 µM. For groups without Piezo1 inhibitors, the same amount of 0.9% NaCl was added to each well 4 hours before vibration. A 6-well plate, a 96-well plate, or a chamber slide was placed on an oscillator with a rubber foam mat and fixed with bands. LFV was applied to the cells in an incubator at 37°C, transmitting mechanical stimuli to the cells in the medium *via* the plate (Figure 1).

2.5. Measurement of intracellular calcium ion levels

To investigate whether vibration stimulation activated the Piezo1 pathway, intracellular Ca^{2+} assays were conducted. The 3T3-L1 cells were seeded into a 96-well culture plate at a density of 1.5×10^4 cells/well. After differentiation and vibration, the intracellular Ca^{2+} concentrations in the 3T3-L1 adipocytes were measured using a Ca^{2+} Measurement Kit (DOJINDO, Kumamoto, Japan) in all groups. Following the manufacturer's protocol, the intracellular Ca^{2+} concentrations were quantified by measuring the fluorescence intensity using a plate reader with an excitation wavelength of 478 nm and an emission wavelength of 518 nm (SpectraMax iD3, Molecular Devices). The relative fluorescence intensity ratio was calculated by normalizing the fluorescence intensity of non-LFV without GsMTx4 group to 1.

2.6. Immunofluorescence staining of GLUT4

The GLUT4 translocation was examined in the fluorescence of GLUT4 following the blockade of the Piezo1 pathway to investigate the relationship between the Piezo1 channel and GLUT4 translocation induced by LFV. The cells were seeded in a chamber slide at a density of 6×10^3 cells/well. After differentiation and vibration, cells from all groups were fixed with 10% formalin for 30 min and subsequently blocked with 1% bovine serum albumin (BSA)/ phosphate-buffered saline (PBS) for 30 min. The cells were washed six times with PBS and then incubated overnight at 4°C with a GLUT4 primary antibody (1:100; polyclonal rabbit antibody, #NBP1-49533, Novus Biologicals, Littleton, CO, USA). After removing the primary antibody, the cells were washed six times with PBS again and incubated with a secondary antibody, Alexa Fluor® 488 (1:1,000; polyclonal donkey antibody, 711-545-152, Jackson ImmunoResearch, West Grove, PA,

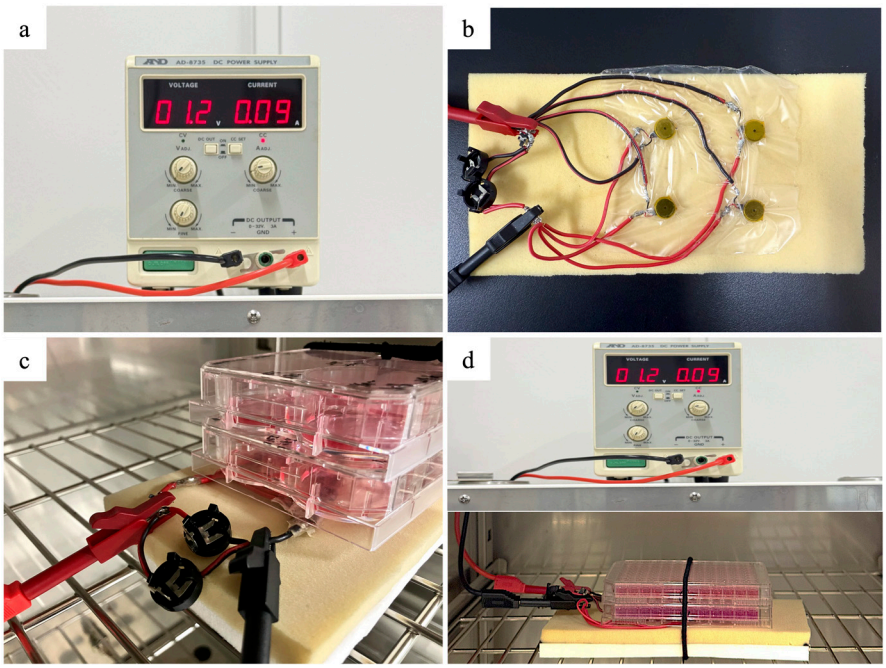

Figure 1. Vibration experimental set-up. a: DC-regulated power supply; **b:** four miniature vibration motors connected in a parallel circuit; **c:** the plate was placed on an oscillator with a rubber foam mat and fixed with bands; **d:** LFV was applied to the cells in a dry heat sterilizer at 37°C, transmitting mechanical stimuli to the cells in the medium *via* the plate.

USA) for 1 h, followed by mounting with DAPI (H-1200-10, Vector Laboratories, Newark, NJ, USA). The GLUT4 fluorescence was observed using a fluorescence microscope (BZ-X810, Keyence, Osaka, Japan).

2.7. 2-Deoxy-D-glucose (2-DG) uptake test

We measured 2-DG uptake while blocking the Piezo1 pathway to elucidate the relationship between the Piezo1 channel and the LFV-induced glucose uptake. A 2-DG Uptake Measurement Kit (Cosmo Bio) was used to evaluate the uptake of glucose in the 3T3-L1 adipocytes in all groups. The cells were seeded in a 6-well culture plate at a density of 6×10^4 cells/well. After differentiation and vibration, adipocytes on day 14 were preincubated in serum-free high-glucose DMEM. 10 µL of a 200 µM GsMTx4 solution in 0.9% NaCl was added to each well GsMTx4 2 h after replacing the medium with serum-free high-glucose DMEM, and then incubated for 4 h. After the total 6-h preincubation, the medium was replaced with 2 mL of Krebs-Ringer phosphate-HEPES buffer (KRPH; 50 mM HEPES, 1.2 mM KH_2PO_4, 137 mM NaCl, 4.8 mM KCl, 1.85 mM $CaCl_2$, and 1.3 mM $MgSO_4$, pH 7.4) containing 2% BSA, and GsMTx4 was added again. The non-LFV group remained in the incubator at 37°C, 5% CO_2, whereas the LFV group was placed in a dry heat sterilizer at 37°C for vibration. After 20 min of vibration, 2-DG (1 mM) was added to both groups, followed by an additional 20 min of incubation or vibration. The cells were subsequently washed three times with PBS and lysed with 1 mL of Tris/HCl buffer (10 mM, pH 8.0). The lysate was collected into tubes, heated to 80°C for 15 min, and centrifuged at 15,000× *g* for 20 min at 4°C. The supernatant was transferred to a new tube and diluted fivefold. The diluted supernatant was combined with each reaction solution according to the manufacturer's instructions. The absorbance of each sample was measured at 420 nm using a plate reader (SpectraMax iD3, Molecular Devices). 2-DG uptake was calculated using a linear plot of the luminescence signal versus the concentration of authentic 2-DG 6-phosphate (µmol/well). The relative ratio was calculated by normalizing the 2-DG uptake of the non-LFV without GsMTx4 group to 1.

2.8. Statistical analyses

All data were presented as the mean ± standard deviation. The differences in the intracellular Ca^{2+} fluorescence intensity and the absorbance of 2-DG between groups were determined using Tukey's multiple comparison test. Statistical analyses were performed using the R software system (version 4.3.3; R Foundation for Statistical Computing, Vienna, Austria). A *p*-value of less than 0.05 was considered statistically significant.

3. Results

3.1. Piezo1 gene expression levels

We confirmed the expression levels of the Piezo1 gene in the 3T3-L1 adipocytes using real-time RT-PCR. All samples exhibited threshold cycle values for *Piezo1* below 30, indicating detectable expression.

3.2. Comparison of intracellular Ca^{2+} fluorescence intensity

The relative intracellular Ca^{2+} fluorescence intensity ratio was significantly higher in the LFV group than in the non-LFV group ($p < 0.0001$). The intracellular Ca^{2+} was significantly lower in the LFV group treated with GsMTx4 than in the LFV group without GsMTx4 ($p < 0.0001$), while the non-LFV group treated with GsMTx4 had no significant difference ($p = 0.590$) (Figure 2).

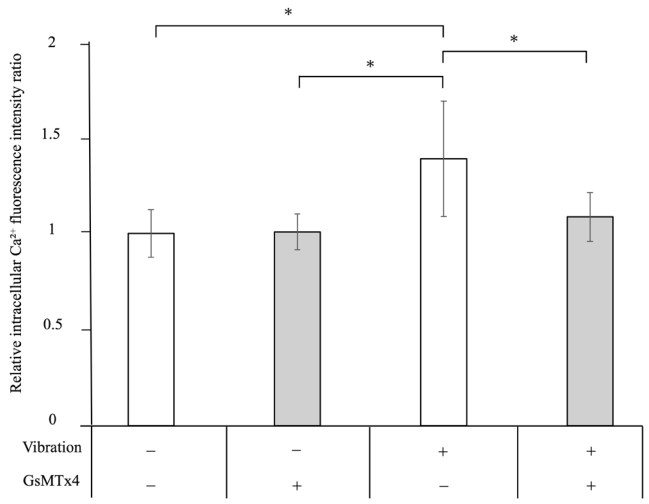

Figure 2. Relative intracellular Ca^{2+} fluorescence intensity ratio under the tested conditions. $n = 18$, *$p < 0.0001$, Tukey's multiple comparison test, means ± standard deviation.

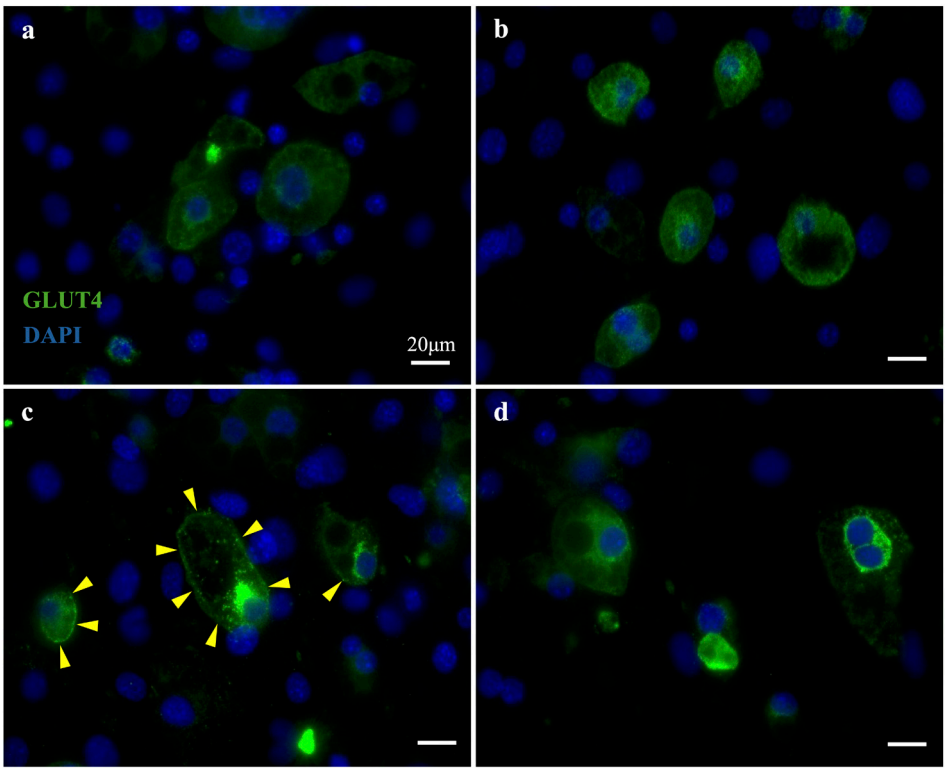

Figure 3. GLUT4 immunofluorescence under the tested conditions. The immunofluorescence staining of GLUT4 under the following conditions: non-LFV groups without GsMTx4 **(a)** and with GsMTx4 **(b)**; LFV groups without GsMTx4 **(c)** and with GsMTx4 **(d)**. In the LFV groups without GsMTx4 (c), the GLUT4 fluorescence was enhanced in the plasma membrane (yellow arrowheads), indicating GLUT4 translocation from the cytoplasm to the plasma membrane by LFV. Scale bar: 20 μm.

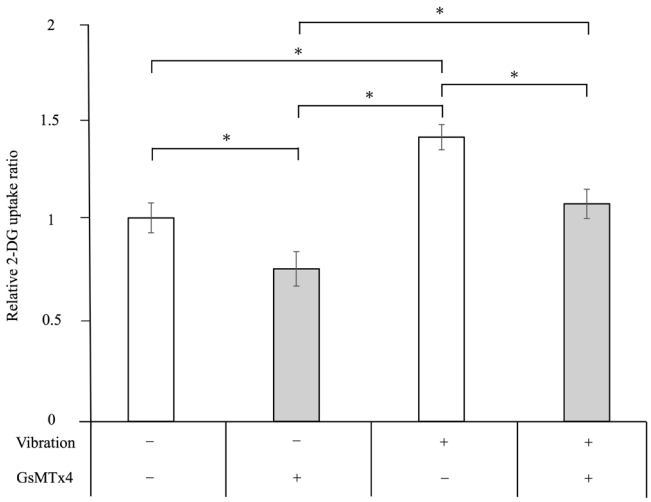

Figure 4. Relative 2-DG uptake ratio under tested conditions. 2-DG uptake in each group was measured in the presence or absence of GsMTx4, and the relative ratio was calculated by normalizing the 2-DG uptake of the non-LFV without GsMTx4 group to 1. ($n = 5$, $*p < 0.01$, Tukey's multiple comparison test, means ± standard deviation).

3.3. Immunofluorescence of GLUT4 under GsMTx4 staining

GLUT4 immunofluorescence staining was performed on the adipocytes from the non-LFV and LFV groups with or without GsMTx4 treatment. Strong GLUT4 fluorescence was observed to be concentrated on the plasma membrane in the LFV group (Figure 3c) compared to the non-LFV group (Figure 3a). In the LFV group treated with GsMTx4 (Figure 3d), GLUT4 fluorescence on the plasma membrane was not as strong compared to the LFV group without GsMTx4 (Figure 3c).

3.4. 2-DG uptake reduced by GsMTx4 treatment

The 2-DG uptake was significantly higher in the LFV group compared to the non-LFV group without GsMTx4 ($p < 0.001$). Moreover, 2-DG uptake was significantly lower

in the LFV group treated with GsMTx4 than in the LFV group without GsMTx4 treatment ($p < 0.001$) However, the 2-DG uptake was also significantly lower in the non-LFV group treated with GsMTx4 compared to the non-LFV group without GsMTx4 ($p < 0.01$) (Figure 4).

4. Discussion

To our knowledge, this is the first report on the effects of Piezo1 on glucose uptake induced by LFV in 3T3-L1 adipocytes. The results of this study demonstrated that LFV stimulated intracellular Ca^{2+} influx, promoted GLUT4 translocation to the plasma membrane, and enhanced 2-DG uptake, which was significantly attenuated by the Piezo1 inhibitor, GsMTx4. These results reveal that Piezo1 is the primary mediator of LFV-induced glucose uptake in 3T3-L1 adipocytes. These findings provide new insights into the mechanistic role of Piezo1 in regulating LFV-induced glucose uptake and metabolism in 3T3-L1 adipocytes. Our findings support the advancement of non-invasive vibration therapy for treating DFUs and encourage the implementation of LFV-based wound care to various clinical settings.

Piezo1, a mechanosensitive ion channel, responds to mechanical stimuli by facilitating the influx of cations, particularly Ca^{2+} (*20-22*). Ca^{2+} influx is an activator of AMPK, a critical regulator of glucose uptake, through the calcium/calmodulin-dependent protein kinase kinase β (CaMKKβ) pathway (*24*). In a previous study, Caco-2 cells (epithelial cells) were subjected to mechanical stretch, which activated the CaMKK2-AMPKα signaling pathway (*25*). This finding of LFV-induced Ca^{2+} influx aligns with the finding in other studies, which used different cell types, where Piezo1 activation was found to initiate calcium signaling pathways (*22,26*).

AMPK plays a central role in energy homeostasis *via* facilitating GLUT4 translocation to the plasma membrane under energy stress or mechanical stimulation (*27*). AMPK-mediated GLUT4 translocation occurs through the transient elevation of the intracellular Ca^{2+} levels or an increased AMP-to-ATP ratio (*28*). In this study, LFV-induced GLUT4 translocation to the plasma membrane was observed. Thus, LFV-induced GLUT4 translocation may potentially be due to AMPK activation *via* Ca^{2+} influx.

In skeletal muscle, exercise or whole-body LFV triggers intracellular Ca^{2+} influx, leading to muscle contraction, AMPK activation, and subsequent glucose uptake *via* GLUT4 translocation (*29,30*). This mechanism parallels the findings of our study, where LFV in adipocytes stimulated Ca^{2+} influx, promoted GLUT4 translocation, and enhanced 2-DG uptake, suggesting that LFV-induced glucose uptake is linked to AMPK signaling.

We primarily focused on the Piezo1-mediated glucose uptake induced by LFV; thus, the potential interplay between Piezo1 and AMPK needs further investigation. Piezo1 activation likely initiates calcium influx, which subsequently triggers AMPK activation. This cascade could provide a mechanistic explanation for the GLUT4 translocation and glucose uptake observed during LFV stimulation. Future studies could examine whether Piezo1 directly modulates AMPK activation through calcium influx, CaMKK, or other intermediary pathways, providing a deeper understanding of the molecular mechanisms underlying LFV-induced glucose metabolism.

Despite these promising findings, several limitations should be acknowledged: First, this study relied solely on GsMTx4, a pharmacological inhibitor commonly used to block Piezo1, to assess its role in calcium influx and glucose uptake. While generally regarded as a selective blocker of mechanosensitive ion channels, GsMTx4 may have off-target effects. Notably, GsMTx4 alone, without LFV, reduced 2-DG uptake, suggesting possible actions on other mechanosensitive channels or related pathways. Therefore, these findings cannot confirm Piezo1 as the sole mediator, and future studies using gene knockdown or knockout approaches are needed. Second, this study used only the 3T3-L1 adipocyte cell line, which is widely applied and well-characterized in adipogenesis and glucose uptake research. Although previous studies have shown that LFV enhances glucose uptake in this cell type (*18*), the *in vitro* system does not fully reproduce the complex biological and physiological environment of primary adipocytes or adipose tissue *in vivo*. Validation using primary adipocytes and animal models, particularly those representing diabetic conditions or diabetic foot ulcers, is needed to confirm the present findings and assess their translational relevance. Third, LFV in this study was tested under only one condition (52 Hz, 600–1,000 mVpp), chosen based on a prior report demonstrating wound-healing effects under these parameters (*17*). While this setting elicited biological responses, the narrow parameter range limits understanding of the dose–response relationship for Piezo1 activation and glucose uptake. Systematic testing of different frequencies, amplitudes, and durations is needed to optimize LFV protocols for potential therapeutic applications. Fourth, other mechanosensitive channels, such as members of the transient receptor potential channel family (*e.g.*, TRPV4, TRPC1), are also known to regulate calcium signaling in response to mechanical stimuli (*31,32*). Although our findings are consistent with Piezo1 involvement, the contribution of these alternative pathways cannot be excluded. Future studies using specific inhibitors or genetic ablation of these mechanosensors are needed to clarify whether Piezo1 is the sole or predominant mediator of LFV-induced effects.

By addressing these limitations in future research, we can more precisely delineate the molecular pathways involved in LFV-induced glucose uptake and strengthen

the translational potential of this approach for metabolic and wound-healing applications.

5. Conclusions

Piezo1 may contribute to glucose uptake induced by LFV in adipocytes, although the involvement of other mechanosensitive channels cannot be ruled out. The key findings are as follows: (i) LFV-induced Ca^{2+} influx in adipocytes is at least partially associated with Piezo1. (ii) Piezo1 contributes to LFV-induced GLUT4 translocation. (iii) Piezo1 is a potential mediator of LFV-induced glucose uptake. Further studies are needed to clarify the involvement of other mechanosensitive ion channels.

Funding: This study was supported by JSPS KAKENHI (grant numbers: 21K18287 and 23H00547) and JST Fusion Oriented Research for Disruptive Science and Technology (FOREST) (grant number: JPMJFR205H).

Conflict of Interest: Dazhuang Huang, Sanai Tomida and Yuko Mugita are affiliated with a department funded by Nichiban Co., Ltd.; Daijiro Haba is affiliated with a department funded by Molten Corporation. However, this study was conducted independently and is unrelated to these sponsors.

References

1. Kolb H, Martin S. Environmental/lifestyle factors in the pathogenesis and prevention of type 2 diabetes. BMC Med. 2017; 15:131.
2. IDF Diabetes Atlas, 10th ed. 2021. https://diabetesatlas.org/ (accessed December 19, 2024).
3. Martinengo L, Olsson M, Bajpai R, Soljak M, Upton Z, Schmidtchen A, Car J, Järbrink K. Prevalence of chronic wounds in the general population: systematic review and meta-analysis of observational studies. Ann Epidemiol. 2019; 29:8-15.
4. Banday MZ, Sameer AS, Nissar S. Pathophysiology of diabetes: an overview. Avicenna J Med. 2020; 10:174-188.
5. Rohm TV, Meier DT, Olefsky JM, Donath MY. Inflammation in obesity, diabetes, and related disorders. Immunity. 2022; 55:31-55.
6. Alavi A, Sibbald RG, Mayer D, Goodman L, Botros M, Armstrong DG, Woo K, Boeni T, Ayello EA, Kirsner RS. Diabetic foot ulcers: Part I. Pathophysiology and prevention. J Am Acad Dermatol. 2014; 70:1.e1-18.
7. Azevedo MM, Lisboa C, Cobrado L, Pina-Vaz C, Rodrigues A. Hard-to-heal wounds, biofilm and wound healing: an intricate interrelationship. Br J Nurs. 2020; 29:S6-S13.
8. Armstrong DG, Boulton AJM, Bus SA. Diabetic foot ulcers and their recurrence. N Engl J Med. 2017; 376:2367-2375.
9. Van Netten JJV, Price PE, Lavery LA, Monteiro-Soares M, Rasmussen A, Jubiz Y, Bus SA. International Working Group on the Diabetic Foot, Prevention of foot ulcers in the at-risk patient with diabetes: a systematic review. Diabetes Metab Res Rev. 2016; 32 (Supplement 1):84-98.
10. Tran MM, Haley MN. Does exercise improve healing of diabetic foot ulcers? A systematic review. J Foot Ankle Res. 2021; 14:19.
11. Basiri R, Spicer M, Levenson C, Ledermann T, Akhavan N, Arjmandi B. Improving dietary intake of essential nutrients can ameliorate inflammation in patients with diabetic foot ulcers. Nutrients. 2022; 14:2393.
12. Hasan R, Firwana B, Elraiyah T, Domecq JP, Prutsky G, Nabhan M, Prokop LJ, Henke P, Tsapas A, Montori VM, Murad MH. A systematic review and meta-analysis of glycemic control for the prevention of diabetic foot syndrome. J Vasc Surg. 2016; 63(Supplement):22S-28S.e2.
13. Nakagami G, Sanada H, Matsui N, Kitagawa A, Yokogawa H, Sekiya N, Ichioka S, Sugama J, Shibata M. Effect of vibration on skin blood flow in an *in vivo* microcirculatory model. BioSci Trends. 2007; 1:161-166.
14. Ichioka S, Yokogawa H, Nakagami G, Sekiya N, Sanada H. *In vivo* analysis of skin microcirculation and the mole of nitric oxide during vibration. Ostomy Wound Manage. 2011; 57:40-47.
15. Sari Y, Sanada H, Minematsu T, Nakagami G, Nagase T, Huang L, Noguchi H, Mori T, Yoshimura K, Sugama J. Vibration inhibits deterioration in rat deep-tissue injury through HIF1-MMP axis. Wound Repair Regen. 2015; 23:386-393.
16. Mahran HG, Helal OF, El-Fiky AAR. Effect of mechanical vibration therapy on healing of foot ulcer in diabetic polyneuropathy patients. J Am Sci. 2013; 9:76-87.
17. Haba D, Ohmiya T, Sekino M, Qin Q, Takizawa C, Tomida S, Minematsu T, Sanada H, Nakagami G. Efficacy of wearable vibration dressings on full-thickness wound healing in a hyperglycemic rat model. Wound Repair Regen. 2023; 31:816-826.
18. Haba D, Nakagami G, Minematsu T, Sanada H. Low-frequency vibration promotes AMPK-mediated glucose uptake in 3T3-L1 adipocytes. Heliyon. 2021; 7:e07897.
19. Haba D, Qin Q, Takizawa C, Tomida S, Minematsu T, Sanada H, Nakagami G. Investigation of ultrasound and low-frequency vibration for glycometabolism promotion in 3T3-L1 adipocytes. Jpn J Electrophysical Agents. 2023; 30:83-92. (in Japanese)
20. Takahashi K, Matsuda Y, Naruse K. Mechanosensitive ion channels. AIMS Biophys. 2016; 3:63-74.
21. Lewis AH, Grandl J. Mechanical sensitivity of Piezo1 ion channels can be tuned by cellular membrane tension. eLife. 2015; 4:e12088.
22. Zhu H, He W, Ye P, Chen J, Wu X, Mu X, Wu Y, Pang H, Han F, Nie X. Piezo1 in skin wound healing and related diseases: mechanotransduction and therapeutic implications. Int Immunopharmacol. 2023; 123:110779.
23. Fei LY, Xu M, Wang HH, Zhong C, Jiang S, Lichtenberger FB, Erdoğan C, Wang H, Bonk JS, Lai EY, Persson PB, Kovács R, Zheng Z, Patzak A, Khedkar PH. Piezo1 mediates vasodilation induced by acute hyperglycemia in mouse renal arteries and microvessels. Hypertension. 2023; 80:1598-1610.
24. Yamashita Y, Jiang H, Okada F, Kitakaze T, Yoshioka Y, Ashida H. Single oral administration of quercetin glycosides prevented acute hyperglycemia by promoting GLUT4 translocation in skeletal muscles through the activation of AMPK in mice. J Clin Biochem Nutr. 2024; 74:37-6.
25. Tao T, Shu Q, Zhao YW, Guo WQ, Wang JT, Shi YH, Jia SQ, Zhai HN, Chen H, Wang CC, Xu GY. Mechanical regulation of lipid and sugar absorption by Piezo1 in

enterocytes. Acta Pharmaceutica Sinica B. 2024; 14:3576-3590.
26. Xie L, Wang XY, Ma YK, Ma H, Shen J, Chen JY, Wang YD, Su SA, Chen KJ, Xu LX, Xie Y, Xiang MX. Piezo1 (piezo-type mechanosensitive ion channel Component 1)-mediated mechanosensation in macrophages impairs perfusion recovery after hindlimb ischemia in mice. Arterioscler Thromb Vasc Biol. 2023; 43:504-518.
27. Bradley H, Shaw CS, Worthington PL, Shepherd SO, Cocks M, Wagenmakers AJM. Quantitative immunofluorescence microscopy of subcellular GLUT4 distribution in human skeletal muscle: effects of endurance and sprint interval 93 training. Physiol Rep. 2014; 2:e12085.
28. Witczak CA, Sharoff CG, Goodyear LJ. AMP-activated protein kinase in skeletal muscle: from structure and localization to its role as a master regulator of cellular metabolism. Cell Mol Life Sci. 2008; 65:3737-3755.
29. Musi N, Hayashi T, Fujii N, Hirshman MF, Witters LA, Goodyear LJ. AMP-activated protein kinase activity and glucose uptake in rat skeletal muscle. Am J Physiol Endocrinol Metab. 2001; 280:E677-E684.
30. Ren Z, Lan Q, Chen Y, Chan YWJ, Mahady GB, Lee SM-Y. Low-magnitude high-frequency vibration decreases body weight gain and increases muscle strength by enhancing the p38 and AMPK pathways in db/db mice. Diabetes Metab Syndr Obes. 2020; 13:979-989.
31. Thodeti CK, Matthews B, Ravi A, Mammoto A, Ghosh K, Bracha AL, Ingber DE. TRPV4 channels mediate cyclic strain-induced endothelial cell reorientation through integrin to integrin signaling. Circ Res. 2009; 104:1123-1130.
32. Maroto R, Raso A, Wood TG, Kurosky A, Martinac B, Hamill OP. TRPC1 forms the stretch-activated cation channel in vertebrate cells. Nat Cell Biol. 2005; 7:179-185.

Received June 30, 2025; Revised August 15, 2025; Accepted August 21, 2025.

**Address correspondence to:*
Gojiro Nakagami, Department of Gerontological Nursing/ Wound Care Management, Graduate School of Medicine, The University of Tokyo, 7-3-1 Hongo, Bunkyo-Ku, Tokyo 113-0033, Japan.
E-mail: gojiron@g.ecc.u-tokyo.ac.jp

Released online in J-STAGE as advance publication August 28, 2025.